PHYSICAL REVIEW B **71**, 094103 (2005)

Structure and stability of hydroxyapatite: Density functional calculation and Rietveld analysis

Donncha Haverty,* Syed A. M. Tofail,† Kenneth T. Stanton,‡ and James B. McMonagle§
Materials and Surface Science Institute, University of Limerick, National Technological Park, Limerick, Ireland

(Received 23 August 2004; published 7 March 2005)

A study on the structure and energetics of hydroxyapatite has been carried out using generalized gradient approximation density functional theory. The previously proposed $P6_3/m$ and $P6_3$ hexagonal structural models have been found to be energetically unfavorable as compared with the previously proposed $P2_1/b$ symmetry and a newly proposed monoclinic $P2_1$ structural model. A detailed analysis of the symmetry restrictions and inconsistencies between the reported physical properties, such as diffraction and birefringence, with hexagonal symmetry question the validity of these models. Rietveld analysis carried out on a synthetic sample, reported to be predominantly hexagonal at room temperature, shows that the diffraction pattern of this material can be interpreted as a mixed monoclinic phase, 23% monoclinic $P2_1/b$ and 77% monoclinic $P2_1$. This interpretation reconciles many anomalies in reported experimental observations.

DOI: 10.1103/PhysRevB.71.094103 PACS number(s): 31.15.Ar, 31.15.Ew, 61.10.Nz, 61.50.Ah

I. INTRODUCTION

Calcium apatites (CaAp) have the general formula $Ca_5(PO_4)_3X$ where X is a negative ion. Apatites are of interest in a number of fields[1] but hydroxyapatite (OHAp) is notably important due to the fact that it is the structural template for the mineral material in human bone and teeth. The structure consists of a pseudo-hexagonal network of PO_4 tetrahedra with Ca^{2+} ions in the interstitial sites and columns of anions oriented along the c axis. Two phases have been suggested based on least square refinements of diffraction data: a disordered hexagonal structure with $P6_3/m$ symmetry (space group 176),[2] and a monoclinic structure with $P2_1/b$ symmetry (space group 14, origin choice 6).[3] The monoclinic unit cell is derived from two hexagonal unit cells with the b parameter twice that of the hexagonal value and involves an ordered arrangement of the anion columns. It has been proposed that the monoclinic phase is associated with stoichiometric apatites.[3]

Fluroapatite, $Ca_5(PO_4)_3F$ (FAp), is known to be hexagonal at room temperature with two formula units per unit cell and is usually taken as a model for the apatite materials.[4] The F^- ions lie at the center of Ca triangles on mirror planes at $z=0.25$ and 0.75. A possible phase transition has been reported at −143.18 °C,[5] the lower temperature phase being a monoclinic arrangement. Chlorapatite, $Ca_5(PO_4)_3Cl$ (ClAp), has the monoclinic structure at room temperature with the Cl^- ions positioned at $z=0.44$ and 0.94.[4] Differential thermal analyses (DTA) studies have shown that ClAp also undergoes a phase transition at 320 °C with the low-temperature phase being monoclinic.[4] The enthalpy for the phase transition was found to be 1.25 J/gm (0.651 kJ mol^{-1}). These results show some correlation with thermally stimulated current (TSC) findings that indicate a relaxation at the temperature of the phase transition.[6]

The structure of hydroxyapatite, $Ca_5(PO_4)_3OH$ (OHAp), has proved more difficult to resolve, but most investigators are content that it is hexagonal $P6_3/m$, since this symmetry gives a good least squares fit to x-ray diffraction (XRD) data.[7,8] This hexagonal structure is usually associated with nonstoichiometric OHAp containing some impurities, e.g., F^- or Cl^-, which give rise to a disordered arrangement of the OH^- ions.[8] In the case of stoichiometric or synthetic OHAp, the structure is expected to adopt a monoclinic ordered arrangement.[3] A reversible enthalpy change at 212 °C has been detected in differential scanning calorimetry (DSC) studies.[9,10] This has been interpreted as the enthalpy change associated with a monoclinic to hexagonal phase transition based on a reduction in the intensities of monoclinic peaks in the experimental diffraction pattern. As with FAp and ClAp, it is suggested that the monoclinic structure is the low-temperature phase. Further evidence of some change in the structure is provided by TSC experiments,[11] which exhibit two relaxations at 211.5 °C. Indirect evidence of a phase change is provided by thermal expansion measurements with the expansion curve showing a change of slope in the region of the transition temperature.[12]

The originally suggested hexagonal $P6_3/m$ OHAp is shown in Fig. 1(a). The central problem associated with this model in the case of OHAp is the reflection of the hydroxyl ions in the mirror planes at $z=0.25$ and 0.75. This leads to the superposition of the oxygen atoms separated by a distance of 0.7 Å. This anomaly is circumvented by assuming that the OH^- ions are disordered with, on average, half the OH ions sitting above the plane of the calcium triangles and half below.[2,7] This necessitates setting the occupancy of these ions to 0.5 for the purposes of structure refinement. However, such a structure must be ordered at least locally in the c direction to avoid electrostatic repulsion between adjacent hydroxyl ions.[7]

If one were to contend that stoichiometric hexagonal hydroxyapatite can exist, then it can only be resolved by removal of the mirror planes at $z=0.25$ and 0.75. This gives rise to the hexagonal space group 173, $P6_3$ symmetry. The loss of symmetry operators on going to the lower symmetry description requires the specification of additional unique atoms: one calcium and one oxygen. This space group gives rise to an ordered structure with the correct number and occupancy of hydroxyl ions. A number of investigators have

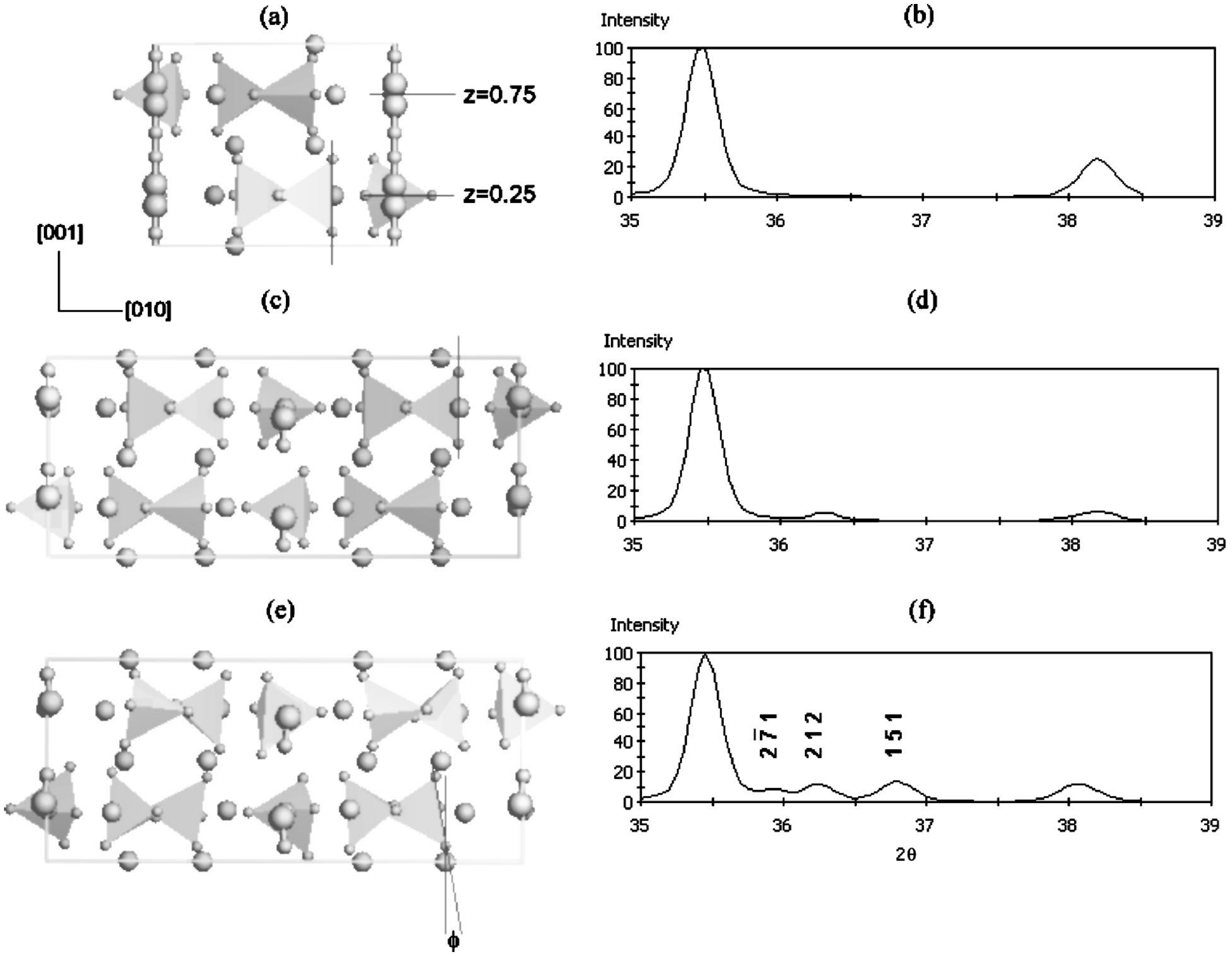

FIG. 1. Various structural models of OHAp and corresponding simulated XRD patterns in the region 35–38.5 °2θ: (a) the disordered $P6_3/m$ structure of Hughes *et al.* (Ref. 8), having the catastrophic superposition of the reflected OH^- ions and the O_3-O_3 edge parallel to the *c* axis; (c) a superstructure with the $P6_3/m$ arrangement of the Ca and PO_4 framework, but with an ordered alternate arrangement of the OH^- ion; (e) the monoclinic $P2_1/b$ structure of Elliot *et al.* (Ref. 3) having a relaxed Ca-PO_4 arrangement in addition to the alternate orientation of OH^- ion. In the latter structure, the origin has been translated to $0,1/4,0$ for ease of comparison. ϕ denotes the extent of relaxation of the O_3-O_3 edge from the $P6_3/m$ positions. (b), (d), and (f) are associated simulated XRD patterns of (a), (c), and (e), respectively.

proposed this symmetry,[1,2,7,13] but its acceptance is limited by the inadequacy of least square fits achieved with this space group.

The previously reported monoclinic structure of Elliot *et al.*[3] is $P2_1/b$. This unit cell was derived from a superstructure comprising two hexagonal unit cells, with every second OH^- column in the *b* direction having alternate orientation. Subsequent least squares refinements distorted the PO_4 tetrahedra, which were no longer constrained as in the high symmetry description.

A previous *ab initio* simulation of OHAp, the first-principles LDA (local density approximation) study of Calderin *et al.*,[14] did not predict any energy difference between the monoclinic and hexagonal phases of OHAp at the static limit. Furthermore, the optimized lattice parameters predicted by the calculations were considerably lower than experimental values, an expected outcome of the LDA approach. The energetics of various OH arrangements using OHAp superstructures with the phosphate framework fixed at the $P6_3$ positions has been investigated by de Leeuw *et al.*[15] In agreement with the suggestion of Sudarsannan *et al.*,[7] they found that the OH ions must be ordered locally in the *c* direction. These investigators also found that the $P2_1/b$ ordered arrangement of hydroxyl columns is lower in energy than the hexagonal $P6_3$ arrangement by 1.3 kJ/mol, but relaxation of the framework was not included in this calculation. It is also worth mentioning that *ab initio* investigations of Posner's cluster $[Ca_9(PO_4)_6]$, the suggested molecular unit involved in the precipitation of OHAp, concluded that the symmetry of the molecular unit is significantly different from the form it takes in crystalline OHAp:[16,17] specifically that the symmetry is lower than the point group associated with the $P6_3/m$ space group.

In the present study we investigate the plausibility of the proposed structural models as well as the feasibility of a monoclinic to hexagonal phase transition, using density functional theory (DFT) superstructure energy calculations carried out at the generalized gradient approximation (GGA) level of theory. We also report a phase analysis of the NIST Standard Reference Material 2910, the purest synthetic

TABLE I. Convergence of lattice parameters and energy with *k*-points sampling set in the case of $P6_3$.

k-points	No. of *k* points	*a* (Å)	*c* (Å)	Energy (eV)
112	2	9.4756	6.8260	−22648.1382
222	4	9.4413	6.8540	−22648.2030
223	8	9.4403	6.8556	−22648.2015

OHAp available[18] for experimental validation of our theoretical arguments.

II. METHODS

A. Computational methods

1. Geometry optimization and energy calculations

As the fundamental difference between the proposed phases of OHAp surrounds the orientation of the hydroxyl columns and given that the OH columns must be ordered locally in the *c* direction, there are two different arrangements to be considered. Thus, calculations were carried out on two superstructures with $P2_1$ symmetry (space group 4, option 2) achieved by doubling the $P6_3/m$ unit cell in the *b* direction: one with the monoclinic $P2_1/b$ alternate arrangement of OH columns, $P2_{1_{\mathrm{ALT}}}$, and the other with the $P6_3$ unidirectional orientation of OH columns, $P2_{1_{\mathrm{UNI}}}$, both ordered structures. The *c* axis is retained as the unique axis for comparison with the hexagonal structures. The superstructure approach ensures consistency of *k*-point sampling and that comparisons are made between structures with similar unit-cell dimensions and composition. In the case of $P2_{1_{\mathrm{ALT}}}$, the optimized structure could always be described by the higher symmetry $P2_1/b$ space group (tolerance <0.05 Å) by translating the origin to 0, 1/4, 0. The optimized $P2_{1_{\mathrm{UNI}}}$ structure could not be described by the $P6_3$ or a higher symmetry space group since the unique angle deviated from 120 deg and the optimized *b* parameter was not exactly twice the *a* parameter. Thus it was necessary to run geometry optimizations on the $P6_3$ structure as it was, to maintain the hexagonal symmetry for comparison with the monoclinic structures.

The total energy package CASTEP (Ref. 30) was used to carry out the density functional theory (DFT) calculations. All geometry optimizations were performed with a BFGS algorithm using the generalized gradient approximation (GGA) functional of Perdew and Wang.[19] 112, 222 and 223 Monkhorst-Pack[20] nets were used to generate the special *k*-point sampling sets in the first Brillouin zone in the case of the $P6_3$ structure. These correspond to sampling sets of two, four, and eight *k* points, respectively. Convergence in the energy and lattice parameters is achieved with a 222 net as shown in Table I. Convergence was also achieved with a 222 net in the case of the superstructures. Ultra soft Vanderbilt pseudopotentials were used to describe the core states[21] and electron-ion interactions. The valence electrons were represented with a plane-wave basis set defined by the kinetic energy cutoff. Variation in the total energy with kinetic energy cutoff (E_{cut}) converged at 750 eV, the value used in all calculations. For the geometry optimizations the following convergence criteria were used: the energy change was less than 2×10^{-5} eV/atom between successive iterations. The rms force tolerance per atom was 50 meV/Å, while the rms displacement and stress tolerances were 0.001 Å and 0.1 GPa, respectively.

2. Rietveld analysis

The computer program DBWS (Ref. 23) was used for least squares fitting of the XRD data to the proposed structures. Least squares refinement was carried out over 615 reflections in the range 25–55 °2θ in the case of the $P2_1/b$ structure and over 687 reflections in the case of the $P2_1$ structure. The background was modeled using a fifth-order Chebyschev polynomial of the first kind. The March-Dollarse method was used to model preferred orientation in the layer plane. The optimized quantum mechanical structures were used as a starting point for the refinements with initial isotropic temperature factors taken from Hughes *et al.*,[8] as were the $P6_3/m$ data. Atomic positions, peak profile, background coefficients, scale factor, and global isotropic temperature factors were allowed to vary during the refinement procedure. Transparency and zero point corrections at the end of the refinement procedure had negligible effect on the *R* values. Except in the case of the disordered $P6_3/m$ model, which necessitated the hydroxyl occupancies to be set to 0.5, the occupancies of all atoms were set to 1.

B. Experimental methods

The NIST standard (SRM 2910)[18] was characterized by x-ray diffraction using a Phillips X'pert PRO MPD X-ray diffractometer (PW3050/60). The copper tube, which operated at 40 kV and 35 mA provided Cu Kα ($\lambda=1.54178$ Å) radiation. The sample (0.5 g) was mounted on a ceramic high-density alumina holder and data collected over the range 24 to 55 °2θ. The step size and dwell time per step were 0.016 °2θ and 600 s, respectively.

III. RESULTS AND DISCUSSION

A. Anomalies of the $P6_3/m$ model

While the hexagonal $P6_3/m$ description may be valid in the case of FAp, the structural model for the apatites, a number of problems can be envisaged when the small spherically symmetric F^- ions, which sit on the mirror planes at $z=0.25$ and 0.75, are replaced by the much larger polar OH^- ions. Within the $P6_3/m$ description there are only three unique tetrahedral oxygens as the anion columns are flanked by PO_4 tetrahedral edges, specifically the edge formed by the two O_3 atoms, using a pseudo-hexagonal terminology based on Hughes[8] proposed $P6_3/m$ structure. The O_3 atoms are symmetry copies of each other via the mirror planes at $z=0.25$ and 0.75, restricting this tetrahedral edge to lie parallel to the *c* axis. Moreover, the *z* parameters of the O_1 and O_2 tetrahedral oxygens are constricted to either 0.25 or 0.75, as these atoms must remain in the mirror planes. In order to accommodate the polar OH^- ion, positioned above or below

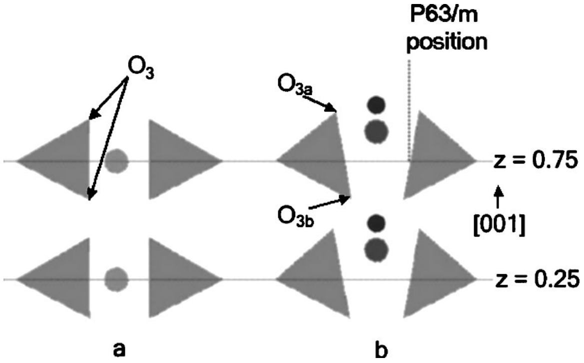

FIG. 2. Schema of the expected phosphate relaxation when the F^- ion (a) is replaced with the polar OH^- ion (b). The schema shows two of the PO_4 tetrahedra surrounding the anions projected onto the (010) plane. In the case of FA the tetrahedral oxygens are labeled as in Ref. 8 In the case of OHAp the oxygens are labeled as in Ref. 3.

the plane, we must expect some perturbation of the PO_4 tetrahedra, with at least some rotation of the O_3-O_3 edge away from its $P6_3/m$ position as illustrated in Fig. 2.

The $P6_3/m$ high symmetry description therefore imposes too many restrictions on the phosphate tetrahedra when the anion is polar or too large to sit in the plane of the Ca triangles. Apart from the fact that disorder is usually associated with high-temperature phases, any disorder in the OH^- ion orientation would also have to be associated with the PO_4 tetrahedra. It has been suggested that impurities such as F^- or Cl^- facilitate the reversal of the OH^- ion orientation in a given column;[2] however, given that it is generally accepted that the stoichiometric material should be monoclinic $P2_1/b$, it is difficult to envisage a situation where the introduction of impurities into such an ideal system would increase the symmetry. In general the perturbation of an ideal system by impurity ions or nonstoichiometry reduces site equivalency and hence the symmetry.

It is illustrative at this stage to look at the theoretical XRD pattern of some structures, as shown in Fig. 1. Figure 1(d) shows the theoretical pattern of a superstructure with the hexagonal $P6_3/m$ arrangement of the phosphate tetrahedra and Ca ions but with the alternate ordered arrangement of the OH^- columns. Figure 1(f) shows the pattern of the monoclinic $P2_1/b$ structure of Elliot *et al.*[3] We can conclude from these patterns that the opposite orientations of adjacent OH^- columns gives rise to an additional (212) x-ray reflection at 36.4 °2θ which is forbidden in hexagonal unit cells. This does not, however, account for all the forbidden reflections observed in this region. It is the relaxation of the phosphate tetrahedra away from their $P6_3/m$ positions that gives rise to the hexagonally forbidden reflections $(2\bar{7}1)$ and (151) at 35.9 and 36.7 2θ, respectively [Fig. 1(f)]. Thus consideration of the OH^- orientation alone is not sufficient to explain the observed experimental pattern. The effect that the displacement of the OH^- ions off the mirror plane has on the surrounding network of tetrahedra cannot be ignored. In order to investigate these effects, a lower symmetry description that does not restrict the framework ions, as in the $P6_3/m$ case, is required. The $P2_1$ superstructures outlined Sec. II A 1 above fulfill this criterion. It should also be noted that while such relaxations can be accommodated within the $P2_1/b$ description, the intensities of the hexagonally forbidden reflections predicted by this structure are greater than those experimentally observed. This may have prompted investigators to retain a $P6_3/m$ component in the phase analysis.[18,24]

B. Geometry optimizations

The optimized $P2_1/b$ (structurally nonpolar) geometry is close to the experimentally determined structure as shown in Table II and this configuration is lowest in energy. The relaxation of the PO_4 tetrahedra in the manner expected to facilitate the OH^- ions in the case of the monoclinic $P2_1/b$ structure is pronounced, with the length of the side of the triangle formed by the phosphate oxygens on the anion side of the (004) plane expanded by 0.41 Å relative to the one below. An interesting feature is that in addition to this rotation of the O_3-O_3 edge away from the $P6_3/m$ position, the reduced symmetry also allows rotation of the O_1-O_2 edge out of the (004) plane, Fig. 3(a). The calculated tetrahedral distortion indices, following the scheme of Baur,[22] are also listed in Table II. It is expected[22] that ortho-phosphates in general would have low indices. As the optimized $P2_1/b$ model has very low Baur indices, the resulting relaxed position of the phosphate tetrahedra can be described as a rotation of the tetrahedra as a whole, away from the $P6_3/m$ position, as opposed to a distortion of one or more of its bonds. A measure of the angle (ϕ) that the O_3-O_3 edge makes with the c axis is an indication of the extent of rotation of the tetrahedra away from the symmetry constrained $P6_3/m$ position, as this edge would lie parallel to this axis in the $P6_3/m$ case. In the case of the $P2_1/b$ structure, $\phi=5.10°$ after averaging over the three unique phosphate groups. This structure is also lowest in energy.

An important feature of the optimized $P2_1/b$ structure is that the tetrahedra can be divided into pairs with each tetrahedron in the pair related through the symmetry operation of the $P2_1$ subgroup. This symmetry operation involves a rotation through 180 deg (C_2) and translation in the [001] direction. In Fig. 3 we show two such pairs and their relationship with the OH^- columns. Imposing a pseudo-hexagonal periodicity on the cell, we could consider the $P6_3/m$ tetrahedral position to be the average of such a pair, as the direction of the rotations of the phosphate tetrahedra away from the $P6_3/m$ position around any OH^- column are related through an opposite congruence, one being positive and one negative. This may explain why the $P6_3/m$ description fits the experimental data so well. In effect, the $P6_3/m$ model can be considered to be a high-symmetry mathematical representation of the monoclinic $P2_1/b$ structure for the purposes of least squares refinement notwithstanding the largely insignificant contribution of the hexagonally forbidden peaks between 35.9 and 38 °2θ. As already discussed, the most plausible physical interpretation of the OH^- disorder is the $P2_1/b$ monoclinic arrangement, and, in relation to the perturbation of the PO_4 tetrahedra, the $P6_3/m$ position represents the average of the $P2_1/b$ positions. Based on neutron diffraction

TABLE II. Lattice parameters and geometries of experimental and GGA predicted structures.

Symmetry	Lattice parameters (Å)	Density (g cm^{-3})	P-O$_m$[a] DI$_{\text{P-O}}$[b]	O-O$_m$[a] DI$_{\text{O-O}}$[b]	O-P-O$_m$[a] DI$_{\text{O-P-O}}$[b]	ΔH_f[c] (kJ mole^{-1})
$P6_3/m$[8]	$a=9.418$	3.16	1.5325	2.5017	109.4400	⋯
	$c=6.875$		0.0019	0.0118	0.0171	
$P6_3$[14]	$a=9.110$	3.30	⋯	⋯	⋯	⋯
	$c=6.860$		⋯	⋯	⋯	
$P6_3$[15]	$a=9.560$	4.07	⋯	⋯	⋯	⋯
	$c=6.830$		⋯	⋯	⋯	
$P6_3$	$a=9.440$	3.13	1.5163	2.4750	109.45	2.579
	$c=6.856$		0.0025	0.0098	0.0152	
$P2_1/b$[3]	$a=9.421$	3.15	1.5358	2.5068	109.4460	⋯
	$b=18.842$		0.0040	0.0102	0.0155	
	$c=6.881$					
	$\gamma=120.00°$					
$P2_1/b$	$a=9.451$	3.15	1.5160	2.4750	109.45	0.00
	$b=18.864$		0.0023	0.0094	0.0139	
	$c=6.852$					
	$\gamma=119.97°$					
$P2_1$	$a=9.450$	3.16	1.5160	2.4750	109.45	1.446
	$b=18.86$		0.0022	0.0096	0.0141	
	$c=6.841$					
	$\gamma=119.86$					

[a] P-O, O-O, and O-P-O refer to the phosphorous oxygen bond length, the tetrahedral edge, and the tetrahedral angle, respectively. The subscript m denotes mean values.

[b] DI refers to the calculated distortion indices (Ref. 22).

[c] The enthalpy of formations, ΔH_f, are given relative to the lowest energy structure, $P2_1/b$.

data, it has previously been suggested[13] that $P6_3/m$ is not the true symmetry of OHAp and represents only the average structure on a macroscopic level.

The optimized geometries of both unidirectional, structurally polar models and their energies relative to the $P2_1/b$ structure are listed in Table II along with the experimental results of Hughes *et al.*[8] ($P6_3/m$) and the calculated values of Calderin *et al.*[14] ($P6_3$) and de Leeuw.[15] Again the indices of the tetrahedra in both symmetry descriptions are low, indicating that the tetrahedra are not significantly distorted although they are slightly more so in the hexagonal structure. The relaxation of the tetrahedra away from the $P6_3/m$ position is not as pronounced as in the $P2_1/b$ case with $\phi=2.0°$ and 2.31° in $P6_3$ and $P2_1$, respectively. The small differences between the $P6_3$ and $P2_1$ descriptions at this stage may seem insignificant enough to disregard the $P2_1$ structure altogether in favor of the hexagonal $P6_3$ description. The $P2_1$ structure is certainly pseudo-hexagonal, but it is lower in energy by 1.33 kJ mole^{-1} than the $P6_3$ description. We will also see that this structure has advantages that come to light in the Rietveld analysis and in the interpretation of the physical properties. Interestingly, it has previously been suggested that $P2_1$ is the correct symmetry description of FA below -143 °C based on electron paramagnetic resonance studies, a technique highly sensitive to local site symmetry.[5]

Regardless of whether the OH$^-$ orientation is polar ($P2_1$ or $P6_3$) or nonpolar ($P2_1/b$), the geometry optimizations show that displacement of the OH$^-$ ions off the mirror planes has a definite effect on the framework tetrahedra in which they are located, namely that the tetrahedra are rotated away from the $P6_3/m$ positions, precluding this space group as the correct symmetry description of OHAp.

C. Rietveld analysis

Rietveld analysis was carried out on the diffraction pattern of the NIST Standard Reference Material 2910 (Ref. 18) using a variety of structural models and mixed phases. The models used and the R values achieved are listed in Table III, the corresponding fits to the experimental data in the narrow region (35–38 °2θ) are shown in Fig. 4. The experimental pattern shows clear evidence of hexagonally forbidden peaks in the narrow region. Furthermore, the worst single-phase fits are obtained with the hexagonal models. It is also evident that the intensities predicted by the $P2_1/b$ model are higher than those observed in the diffraction pattern as was in general previously found to be the case.[18,24] On the other hand, the best single phase overall fit is achieved with the monoclinic $P2_1$ structure and, in particular, this model shows excellent correlation with the diffraction pattern in the narrow region with the $(\overline{27}1)$, (212), and (151) peaks being intermediate in intensity between zero, in the case of the hexagonal models, and the high values predicted by the $P2_1/b$ model.

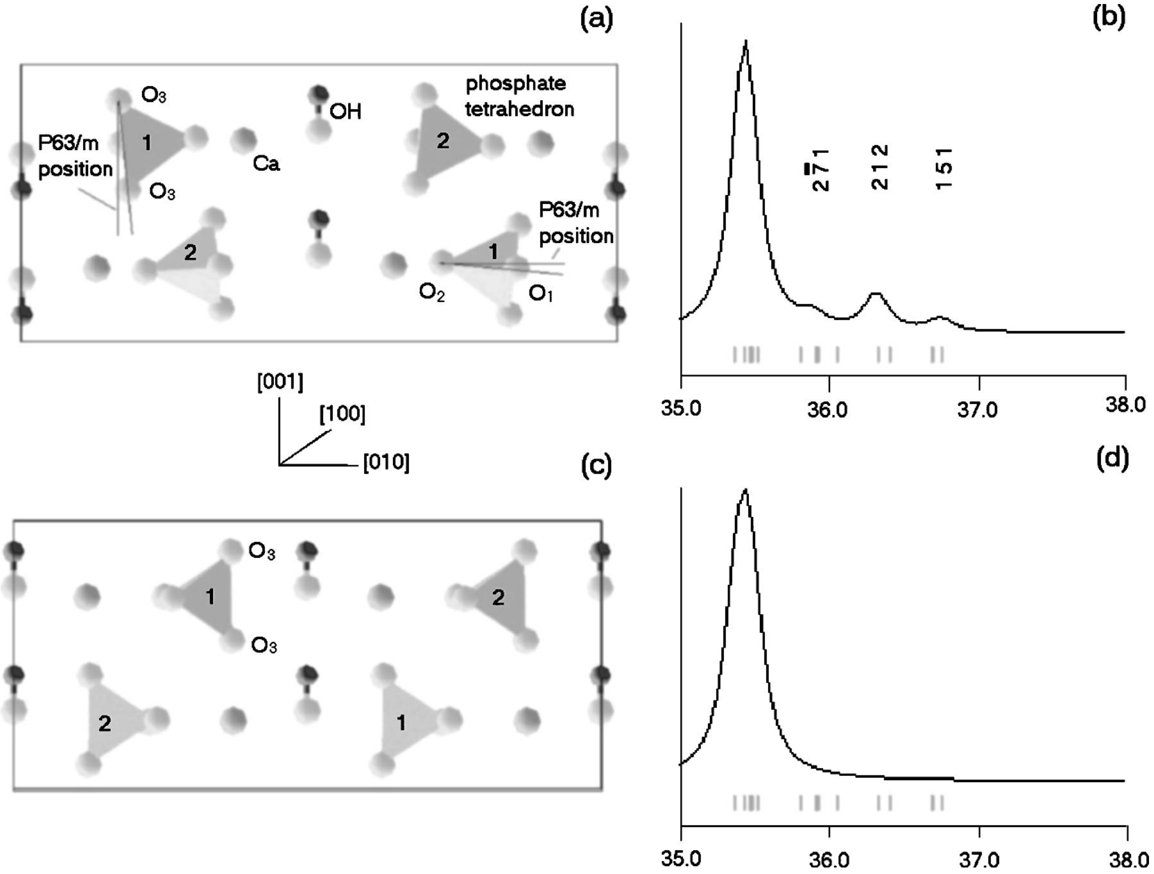

FIG. 3. The relationship between two pairs of tetrahedra and hydroxyl column orientation for the optimized $P2_1/b$ structure (a), its simulated XRD pattern (b), the optimized $P2_1$ structure (c) and the corresponding simulated XRD pattern (d). Tetrahedra that are symmetry copies of each other via the $P2_1$ symmetry operation are numbered similarly. In order to accommodate the polar OH^- ion, both the O_3-O_3 and O_1-O_2 edges the phosphate tetrahedra in question should rotate away from their $P6_3/m$ positions. The O_3-O_3 edge rotation and O_1-O_2 edge rotation from their respective $P6_3/m$ positions are shown in (a). In the simulated XRD pattern of the $P2_1/b$ description, the hexagonally forbidden reflections at 35.9, 36.7, and 36.4 $°2\theta$ are indexed $(2\overline{7}1)$, (151), and (212), respectively. The $(2\overline{7}1)$ and (151) reflections are associated with the phosphate tetrahedral rotations while the ordered alternate arrangement of the hydroxyl columns gives rise to the (212) reflection. The relaxation of the phosphate tetrahedra is more pronounced in the $P2_1/b$ model, with the length of the side of the triangle formed by the phosphate oxygens on the anion side of the mirror planes expanded by 0.41 Å relative to the one below.

In both monoclinic structures there was a tendency for the hydroxyl oxygen to move from its hexagonally constrained position within the pseudo-basal plane. Although XRD cannot be relied on for the hydrogen position, this is indicative of the OH^- bond axis being tilted slightly from the [001] direction. Furthermore, the rotations of the three phosphate tetrahedra surrounding a given OH^- ion were such that one of the O_3-O_3 edges was rotated towards the OH^- ion while the others were rotated away from the OH^- ion. This may indicate some form of weak interaction between the hydroxyl hydrogen and one of the phosphate oxygens that was not revealed in the *ab initio* calculations, perhaps as a result of using a bare Coulomb potential to describe the hydrogen. Such rotations of the tetrahedra relative to one another cannot be accommodated within the hexagonal symmetry descriptions where there is only one unique tetrahedron. It was with such an arrangement of the phosphate groups within the $P2_1$ symmetry description that the best single phase fit to the experimental pattern was achieved.

It has been common practice to interpret OHAp as a mixture of $P2_1/b$ and $P6_3/m$ to yield the required intensities in the narrow region.[18,24] However, with the present work concluding that $P6_3/m$ is not a valid symmetry description of OHAp, a phase analysis with $P2_1/b$ and $P2_1$ components seems more appropriate. Such an analysis gives the best fit to the diffraction pattern and suggests that the NIST standard reference material is 77% monoclinic $P2_1$ and 23% monoclinic $P2_1/b$.

These results underline the limitations of the least square refinement method for resolving fine structural detail. In cases where empirically modeled disorder theories are warranted, they should be used with caution. It seems in the case of OHAp that the disorder theory was introduced to circumvent the anomaly of the superposition of the hydroxyl ions reflected in the mirror planes. This arose as a consequence of assuming that the symmetry would be unchanged when the F ion of FAp (the structural model for the apatites) was replaced by the OH ion, which is neither spherically symmetric nor small enough to sit in the mirror planes within the apatitic framework. That this empirical remedy gives such a good match to the experimental pattern highlights the need to be prudent when using least square analysis. In cases where

TABLE III. R-factors and geometries of phases fit to SRM 2910 over the range $24-55\,°2\theta$.

Label in Fig. 4	Phase/s	Lattice parameters a,b,c, (Å) and γ		R_p	R_{wp}
a	$P6_3/m$ 100%	$a=9.419$	$c=6.88$	2.85	3.68
b	$P6_3$ 100%	$a=9.419$	$c=6.88$	2.69	3.48
c	$P2_1/b$ 100%	$a=9.415$	$b=18.826$	2.66	3.47
		$c=6.88$	$\gamma=119.87°$		
d	$P2_1$ 100%	$a=9.415$	$b=18.846$	2.43	3.17
		$c=6.88$	$\gamma=119.89°$		
e	$P2_1$ 77.4%	$P2_1$	$P2_1/b$	2.13	2.82
	$P2_1/b$ 22.6%	$a=9.413$	$a=9.413$		
		$b=18.84$	$b=18.83$		
		$c=6.88$	$c=6.88$		
		$\gamma=119.89°$	$\gamma=119.87°$		

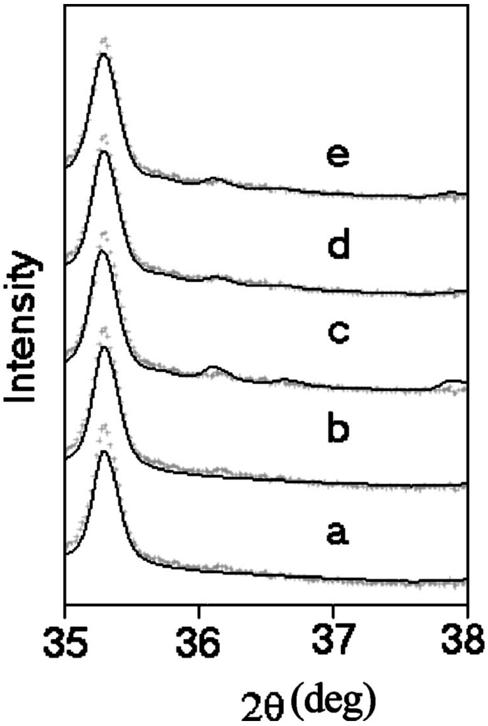

FIG. 4. The Rietveld fits of various structural models to the experimentally measured pattern of the polycrystalline NIST standard in the region $35-38\,°2\theta$ are shown. The phases and associated labels are listed in Table III.

a number of different models give comparable least square fits, the energy and structural information provided by *ab initio* simulation provides a powerful tool to probe the finer detail of a structure, but one must also look to physical properties (other than diffraction) and reconcile the predicted crystal symmetry with the symmetry suggested by experimental observation.

D. Physical implications

Previous investigators who have tried to interpret the observed physical properties of OHAp, in particular the relaxation phenomena observed in thermally stimulated current[11] (TSC) studies have only considered OH^- reorientation and ignored the role of the framework tetrahedra in these processes. Our calculations indicate that the most likely phase transition, from the alternate OH^- orientation, $P2_1/b$, to the unidirectional orientation, $P2_1$, must be accompanied by a relaxation of the framework tetrahedra specifically, a rotation of the tetrahedra as opposed to a distortion of their bonds. This may explain the observation of two relaxations with different activation energies at 211.5 °C in the TSC studies, one being associated with the OH^- ion reorientation and the other with the accompanying phosphate tetrahedral rotation. Such reorientation of the OH^- ions and rotation of the PO_4 tetrahedra have interesting consequences for the XRD pattern. Figures 3(b) and 3(d) show the theoretical XRD patterns in the region where the most intense hexagonally forbidden reflections appear ($35-38\,°2\theta$). There is a substantial decrease in the intensities of these reflections on going from the monoclinic $P2_1/b$ structure to our hypothesized monoclinic $P2_1$ structure (they are forbidden in the $P6_3$ description). The observation of biaxial birefringence beyond the transition temperature has questioned the proposition of the high temperature phase being hexagonal.[4] However, the enthalpy changes[9,10] and dielectric relaxations[25–28] observed in the vicinity of 212 °C taken with the marked reduction in the intensity of the hexagonally forbidden reflections do point to some structural change at 212 °C. We suggest that the phase transition is not to a hexagonal structure at all, but to another monoclinic arrangement, $P2_1$, explaining the observation of birefringence beyond the transition temperature.

The absence of a center of symmetry in the $P2_1$ represents a substantial difference between it and $P2_1/b$, or indeed $P6_3/m$, particularly in relation to the dielectric properties of OHAp. It is clear from the TSC and thermally stimulated depolarization current (TSDC) studies that polar relaxations do occur in OHAp when the initial polarization temperature is above the phase transition temperature.[25,28] This suggests that OHAp is pyroelectric and, theoretically at least, piezoelectric. However, the broadness of the relaxation peaks in OHAp as compared with those observed in typical ferroelectric materials suggest that the relaxation phenomena in OHAp are very distinct and, in particular, very slow. Nakamura[25] have shown that the TSDC spectra of polarized OHAp, cooled to room temperature and short-circuited, remain the same after 60 days. Most investigators explain the relaxations in terms of OH^- displacements or migration of the hydroxyl hydrogen. These being the only considerations, one would expect the polarization of OHAp to be easily reversed, but this does not seem to be the case. Our work suggests that the kinetically hindered polarization phenomena and the relatively high polarization temperatures required in OHAp arise because not only are the OH^- ions displaced/reoriented, but there must also be a large activation energy supplied to rotate the phosphate tetrahedra. It is most likely this reorientation of the OH^- columns coupled with the phosphate tetrahedral rotation that gives rise to the peculiar dielectric properties of OHAp. Furthermore, if the transition were to the paraelectric $P6_3/m$ phase, the dielectric permittivity should follow the Curie-Weiss law, which is not what is observed in practice.[26,27] It may be the activation energy associated with rotating the tetrahedra that stabilizes the polar phase at room temperature in the polycrystalline material. Empirical calculations[29] that used an ordered unidirectional model suggest a link between crystallite size and surface energy. At small slab thickness (c direction) the surface energy was low, but above 2 nm thickness there was a considerable increase to a relatively constant value. It is worth noting that the only convincing XRD evidence suggesting an appreciable monoclinic $P2_1/b$ phase [2,3,5] was achieved using single crystals where the surface effect is negligible. In the case of the polycrystalline material, however, the surface effect is large and a possible gain in surface energy terms might favor the $P2_1$ unidirectional orientation. Indeed it is reasonable to suggest that the surface provides the site for initiating OH^- column reorientation during the phase transition. Furthermore, the morphology of OHAp in bone is thin platelets in the range of 2–4 nm, and it is well known that bone is piezoelectric. Although the origin of this property is a matter of some debate, it is a phenomenon requiring the absence of a center of symmetry, as in the $P2_1$ structure. It may well be that the desirable properties of OHAp, namely its properties *in vivo*, arise as a consequence of the dielectric properties associated with the non-centrosymmetric $P2_1$ phase.

IV. CONCLUSIONS

A close examination of the structure and energetics of hydroxyapatite has highlighted serious shortcomings in the validity of hexagonal structural models for this material. DFT calculations have shown both the $P6_3/m$ and $P6_3$ structures to be energetically unfavorable in comparison with monoclinic models. A detailed examination of XRD pattern fine structures, generated both from experimental analysis and simulated structural models, has shown that $P6_3/m$ symmetry is untenable as a basis for the structure of OHAp.

Two monoclinic models, having the previously proposed $P2_1/b$ symmetry[3] and a novel $P2_1$ symmetry, have been found to give structural descriptions of this material that are most consistent with the observed physical properties and predicted energetics. In the case of the $P2_1/b$ model, detailed geometry optimization analysis of the simulated XRD pattern fine structure revealed both the existence of an ordered alternate OH^- arrangement and a hitherto unreported relaxation of the phosphate tetrahedral away from the $P6_3/m$ position.

Rietveld analyses carried out on the experimentally obtained diffraction pattern from a synthetic standard reference material OHAp sample indicated it to comprise a mixture of the $P2_1$ (77%) and $P2_1/b$ (23%) phases.

Reconciliation of the present results with previously reported work (TSC,[11] TSDC,[25,28] and birefringence[4] studies) on the OHAp phase transition observed at 211.5 °C, strongly suggests that this transition occurs from the nonpolar (alternate OH^- orientation) $P2_1/b$ phase to the newly proposed polar (unidirectional OH^- orientation) $P2_1$ phase. TSC studies[11] which have reported the occurrence of two relaxations at the phase transition temperature may be interpreted in the light of the present work as resulting from OH^- reorientation and accompanying phosphate tetrahedron rotation processes. An explanation is also proposed for the unusually broad nature of these relaxation peaks, indicative of kinetically hindered polarization phenomena: overall large activation energies accruing as a result of these coupled reorientation and rotation processes.

The absence of a center of symmetry in the polar $P2_1$ structure points towards pyroelectric and potential piezoelectric properties for this OHAp phase. In the case of the latter property, it is thought that OHAp in polycrystalline or thin platelet form (as it occurs in bone) may be best described by the energetically favorable $P2_1$ phase. This may in turn shed light on the observation of bone piezoelectricity and the *in vivo* bonding properties of OHAp.

---

*Electronic address: donncha.haverty@ul.ie
†Electronic address: tofail.syed@ul.ie
‡Electronic address: kenneth.stanton@ul.ie; Also at: Department of Mechanical Engineering, University College Dublin, Belfield, Dublin 4, Ireland.
§Electronic address: seamus.mcmonagle@ul.ie

[1] D. McConnell, *Apatite* (Springer-Verlag, Wien, 1973).
[2] M. I. Kay, R. A. Young, and A. S. Posner, Nature (London) **204**, 1050 (1964).
[3] J. C. Elliot, P. E. Mackie, and R. A. Young, Science **180**, 1055 (1973).
[4] J. C. Elliot, *Structure and Chemistry of the Apatites and Other Calcium Phosphates* (Elsevier, Amsterdam, 1994).
[5] M. Greenblatt and J. H. Pifer, J. Chem. Phys. **66**, 559 (1977).
[6] N. Hitmi, C. LaCabanne, and R. A. Young, J. Phys. Chem. Solids **45**, 701 (1984).
[7] K. Sudarsanan and R. A. Young, Acta Crystallogr., Sect. B: Struct. Crystallogr. Cryst. Chem. **B25**, 1534 (1969).
[8] J. M. Hughes, M. Cameron, and K. D. Crowley, Am. Mineral. **74**, 870 (1989).
[9] H. Suda, M. Yashima, M. Kakihana, and M. Yoshimura, J. Phys. Chem. **99**, 6752 (1995).
[10] H. Takahashi, M. Yashima, M. Kakihana, and M. Yoshimura, Thermochim. Acta **371**, 53 (2001).
[11] N. Hitmi, C. LaCabanne, and R. A. Young, J. Phys. Chem. Solids **49**, 541 (1988).
[12] S. Nakamura, R. Otsuka, H. Aoki, M. Akao, N. Miura, and T. Yamamoto, Thermochim. Acta **165**, 57 (1990).
[13] A. T. Sanger and W. F. Kuhs, Z. Kristallogr. **199**, 123 (1992).
[14] L. Calderin, M. J. Scott, and A. Rubio, Phys. Rev. B **67**, 134106 (2003).
[15] N. H. de Leeuw, Phys. Chem. Chem. Phys. **4**, 3865 (2002).
[16] G. Treboux, P. Layrolle, N. Kanzaki, K. Onuma, and A. Ito, J. Am. Chem. Soc. **122**, 8323 (2000).

[17] G. Treboux, P. Layrolle, N. Kanzaki, K. Onuma, and A. Ito, J. Phys. Chem. A **104**, 5111 (2000).

[18] E. J. Amis and J. Rumble, *Certificate of analysis, SRM 2910: Calcium hydroxyapatite* (National Institute of Standards and Technology, Gaithersburg, MD, 2003).

[19] J. P. Perdew and Y. Wang, Phys. Rev. B **45**, 13 244 (1992).

[20] H. Monkhorst and J. Pack, Phys. Rev. B **13**, 5188 (1976).

[21] D. Vanderbilt, Phys. Rev. B **41**, 7892 (1990).

[22] W. H. Baur, Acta Crystallogr., Sect. B: Struct. Crystallogr. Cryst. Chem. **B30**, 1195 (1974).

[23] D. B. Wiles and R. A. Young, J. Appl. Crystallogr. **14**, 149 (1981).

[24] H. Morgan, R. M. Wilson, J. C. Elliot, S. E. P. Dowker, and P. Anderson, Biomaterials **21**, 617 (2000).

[25] S. Nakamura, H. Takeda, and K. Yamashita, J. Appl. Phys. **89**, 5386 (2001).

[26] N. A. Zakharov and V. P. Orlovskiĭ, Tech. Phys. Lett. **27**, 629 (2001).

[27] V. P. Orlovskiĭ, N. A. Zakharov, and A. A. Ivanov, Inorg. Mater. **32**, 654 (1996).

[28] I. M. Kalogeras, A. Vassilikou-Dova, and A. Katerinopoulou, J. Appl. Phys. **92**, 406 (2002).

[29] W. T. Lee, M. T. Dove, and E. K. H. Salje, J. Phys.: Condens. Matter **12**, 9829 (2000).

[30] Accelrys Inc., 9685 Scranton Road, San Diego, CA 92121-3752, USA.